Power MOSFET based Photo-Voltaic Battery Charger Analysis and Implementation

Kamala J, Janarthanan V, and Santhosh K

***Abstract*—** Power MOSFET is the basic control element in all types of power electronic converters. Recent studies are focused on charging Battery using Solar Energy to eliminate the energy crisis. This paper analyzes the losses associated with Power MOSFET used to charge batteries from solar energy. N channel and P channel HEXFET Power MOSFET Devices are chosen. Efficiency of the Photo-Voltaic (PV) charger is derived for different switching frequencies of device. Efficiency of PV system with N channel device is better with complicated gate driver circuit, compared to P channel device. Solar panel of 100W and battery of 12V, 42Ah capacity is chosen for this application. Maximum power point voltage of solar cells occurs at 17.5V. Direct controlled connection between solar cell and battery is one method of battery charging. Second approach uses Buck converter to charge the battery. Both techniques use power MOSFET for control purpose. Parameters available for controller for this application are Solar panel voltage/current and Battery voltage/current. As the battery voltage is fixed, it is shown that sensing battery current for control purpose provides better results compared to usual Maximum Power Point Tracking (MPPT) algorithms. Spartan 6 Field Programmable Gate Array (FPGA) based battery charge controller is implemented based on the results of this paper. Results and discussions of this paper are useful for the selection of switching device, duty cycle and the operating frequency.

***Keywords*—** Buck converter, Filed Programmable Gate Array, Power MOSFET, Switching losses, Transfer characteristics.

I. Introduction

PHOTO-VOLTAIC energy storage system uses DC-DC converters with MPPT algorithm for maximum energy transfer [1]. MPPT algorithms use solar panel voltage and current to locate maximum power point. Maximum power is delivered to load by MPPT based controllers [2-6]. In a battery charging system, source voltage of N-MOSFET is fixed at battery voltage. Therefore, conventional MPPT algorithm does not deliver maximum current for battery charging [7]. This paper analyses losses involved in the power device by applying switching signals at different frequencies and duty cycles. Detailed analysis of MOSFET characteristics in a photo-voltaic system is required to find the switching requirements. Transfer characteristics of the device indicate the gate drive requirement for switching. It is derived by connecting the power MOSFET between solar panel and battery, with various gate voltages, as shown in figure 1. In this case, battery charging is possible only if solar panel voltage is sufficiently greater than battery voltage. N channel and P channel HEXFET Power MOSFET characteristics curves are obtained with battery load. Simple battery charging circuit can be easily designed using power MOSFET between solar panel and battery.

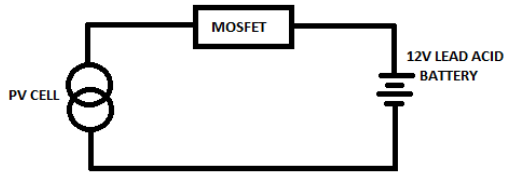

Figure 1 Power MOSFET coupled between PV cell and battery

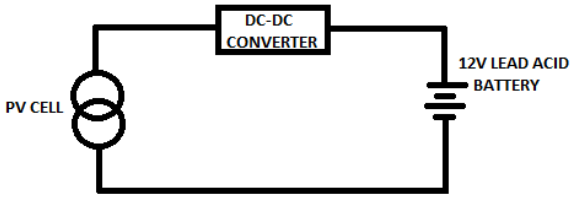

Figure 2 Battery charging through power converter

Efficiency of battery charging system is improved by connecting DC-DC converter between solar panel and battery. If battery voltage does not match with solar panel specifications, suitable DC-DC converter is used. Boost converter is used if battery voltage is greater than solar panel voltage [8-10]. Buck converter is used, if battery voltage is less than solar panel voltage. It consists of inductance, capacitance and power electronic semi-conductor devices [3]. Inductor and capacitor sizing is decided by switching frequency of power electronic components. Higher frequency leads to smaller values of inductor and capacitor with improved output regulation [11-15]. Power electronic components are designed with low on state resistance, fast switching rate, higher voltage and current carrying capacity [16]. Efficiency of converter depends on the losses of power MOSFET and converter. It is analyzed for various switching frequencies applied to different configurations of switching devices. In this work, solar panel is connected to battery through buck converter as shown in figure 2. Buck controller is easily controllable and stable DC_DC converter [8,17]. FPGA is chosen to generate PWM signals of

This work is funded by the Centre for Technology Development and Transfer, Research Support Scheme of Anna University, Chennai, Tamil Nadu, India.

J. Kamala is with College of Engg. Guindy, Anna University, Chennai, Tamil Nadu (phone: 91-044-22358898; e-mail: jkamalaa@annauniv.edu, jkamalaa06@gmail.com).

V. Janarthanan and K. Santhosh were with College of Engg. Guindy, Anna University, Chennai, Tamil Nadu (e-mail: jana6023@gmail.com, lksanthosh00@gmail.com).

converter. It supports fast and parallel execution of complex algorithms with easier programming techniques. [11,12,18].

Photo-voltaic energy storage system with a solar panel of $100W_p$, V_{mp} of 17.5V, I_{mp} of 5A and a battery of 12V, 42Ah are considered in the proposed research work. Section II describes overall photo-voltaic charging system and its hardware specifications. Section III discusses the transfer characteristics of power electronic components connected between solar panel and battery. Converter efficiency is analyzed in section IV for various switching frequencies applied to different devices. Section V discusses the results obtained with the experimental set-up and controller implementation using FPGA. Section VI concludes with the power component requirements and its characteristics applied to battery charging.

II. PHOTO-VOLTAIC BATTERY CHARGING SYSTEM

Specifications of solar panel are given in Table 1. Solar panel peak voltage is greater than rated battery voltage. Therefore battery charging is achieved either by connecting switch between solar panel and battery as shown in figure 3 or by using Buck converter as shown in figure 5. PWM generator output circuit controls the switching device according to the battery charge state.

TABLE 1 SPECIFICATIONS OF SOLAR PANEL

Characteristics	Specification
Rated power, P	100Wp
Peak power voltage, V_{mpp}	17.5V
Peak power current, I_{mpp}	5A
Open circuit voltage, V_{oc}	21.4V
Short circuit current, I_{sc}	6A

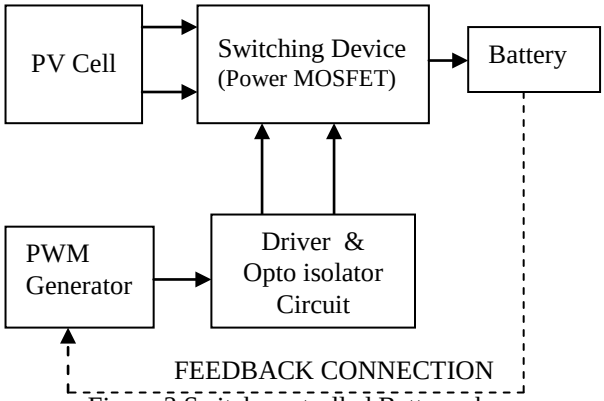

Figure 3 Switch controlled Battery charger

HEXFET Power MOSFET devices are used as switching devices. They are voltage controlled devices, which require a voltage between gate and source terminal for current to flow in the drain terminal [19-22]. System performance is monitored for both N and P channel devices. Important parameters of the switching devices are given in Table 2

Table 2 Switching Device Parameters

IRFP150N – N channel	IRF9530 – P channel
MOSFET	MOSFET
$V_{GS(th)}$ = 2 to 4V	$V_{GS(th)}$ = -2 to -4V
V_{DSS} = 100V	V_{DSS} = -100V
$R_{DS(on)}$ = 0.036Ω	$R_{DS(on)}$ = 0.2Ω
I_D = 42A	I_D = -14A

Charge pump circuit is required for gate of N channel MOSFET, which is achieved by a driver and opto-isolator circuit. Complementary pair switching transistors 2N2907A and PN2222A are used to improve the drive strength of signal. Opto-isolator TLP250 is used for isolation [23].

Buck converter capable of handling 500W is designed with the following requirements

- Switching frequency = 1 MHz maximum
- Current ripple < 0.04A
- Voltage ripple < 0.01V
- Charging current = 10A maximum
- Duty cycle = 5% to 95%

Specifications of converter are given as follows and shown in figure 4

- Input voltage : varies between 14V-20V
- Output voltage : 11V – 14.5V (Battery no load threshold limits)
- MOSFET : IRFP150N / IRF 9530
- Diode : MBR1545
- Inductance : 100µH
- Capacitance: 1000µF

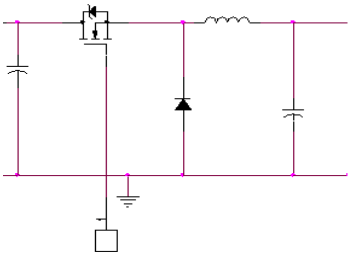

Figure 4 Buck Converter

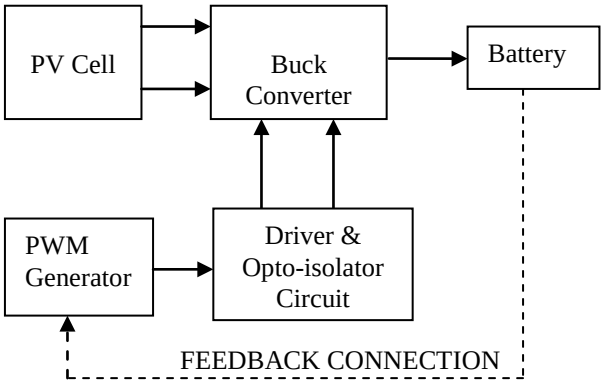

Figure 5 Converter based Battery charger

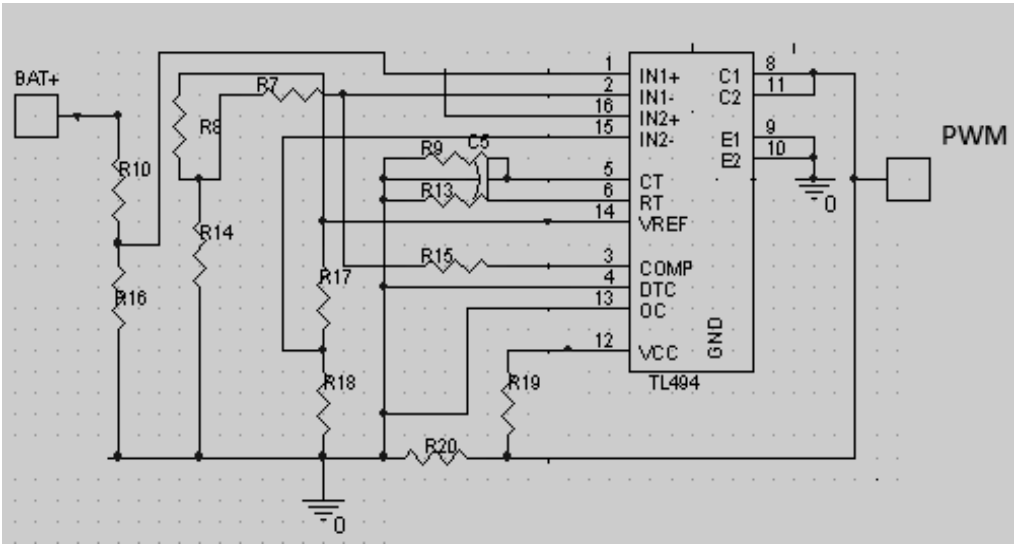

Figure 6 PWM Generation circuit

TL494 pulse width modulator IC is used to generate the PWM signal of converter. Battery voltage is fed back to PWM generator circuit using potentiometer, that can be adjusted to vary the duty cycle of PWM signal. Frequency of PWM signal is varied by varying the resistance of oscillator circuit. Circuit shown in figure 6 uses resistance R13(potentiometer) to vary frequency and R16 to adjust the duty cycle

III. MOSFET Transfer Characteristics coupled between PV Cell and Battery

HEXFET N channel power MOSFET IRFP150N and P channel device IRF9530 are chosen to study the transfer characteristics. Connection of MOS devices between PV cell and battery is shown in figure 7.

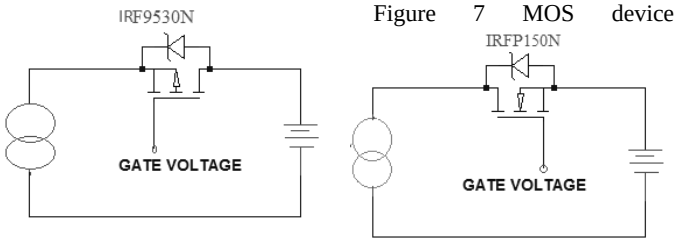

Figure 7 MOS device connected between PV cell and battery

Flow of drain current charges the battery and increases battery voltage with drain to source voltage decreasing from 7V to 0.15V. Maximum drain current is 5.36A with single N channel MOS device and it is increased to 5.41A with two devices in parallel. Parallel connection of devices reduces on-resistance of device and increases drain current. Drain current flow with gate to source voltage and drain to source voltage is shown in figure 8.

Flow of drain current charges the battery and increases battery voltage with drain to source voltage decreasing from 7V to 0.15V. Maximum drain current is 5.36A with single N channel MOS device and it is increased to 5.41A with two devices in parallel. Parallel connection of devices reduces on-

Figure 8 Characteristics of NMOS device

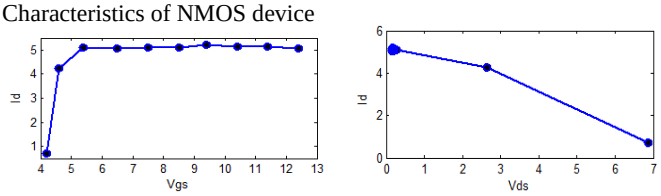

resistance of device and increases drain current. Drain current flow with gate to source voltage and drain to source voltage is shown in figure 8.

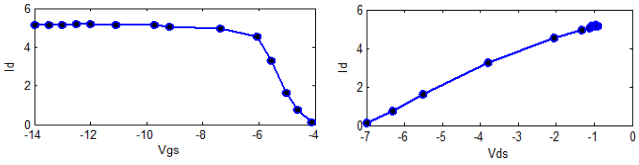

Figure 9 Characteristics of PMOS devices

In case of P channel devices, gate voltage need not be higher than source. Gate signal can be derived from the input signal and charge pump circuit is not required. On-resistance of P channel MOS is higher and drain current is comparatively reduced. Maximum drain current for this case is 5.16A with single device and 5.3A with two devices in parallel. Characteristic curves of PMOS device is shown in figure 9.

Battery can be charged by applying a constant voltage to gate terminal to switch on power MOSFET. Control circuit is added to maintain output terminal at constant voltage or current. The device is in continuous conduction state and conduction loss of the device is involved. This type of system is classified into linear regulators, which has poor efficiency. Switching regulators called converters are used for better efficiency. Converter performance with different combinations of Power MOSFET devices is discussed in the following section.

Figure 10 Efficiency of converter with different MOS devices

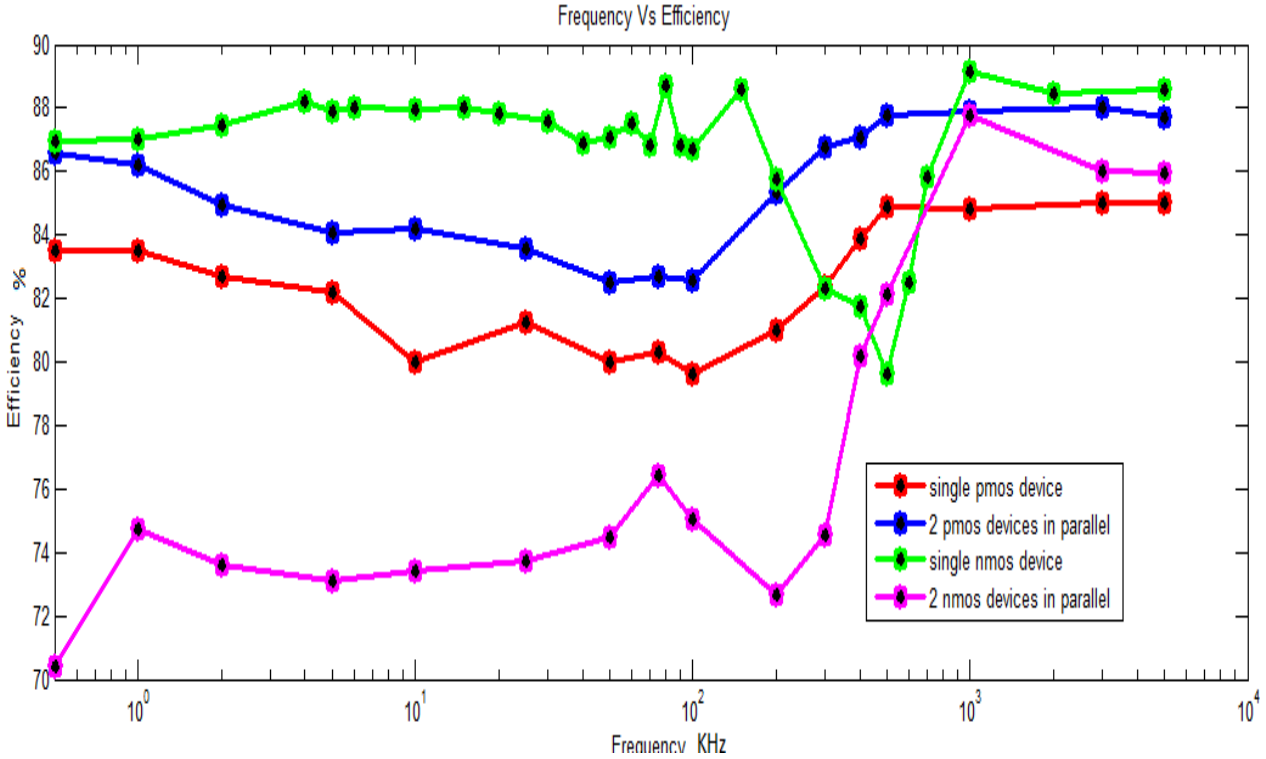

IV. Converter Performance with MOS Devices

Battery charging depends on the current flow. Higher current flow enables faster battery charging. Conventinal MPPT is not effective for battery charging system, since the output voltage is fixed at battery voltage, which is not V_{mp} of PV cell. This paper analyzes the efficiency of converter by varying switching frequency for different MOSFET configurations. Input / output measurements of converter is taken for four cases of power electronic component connections as given below

- Single N channel power MOSFET
- Two N channel power MOSFETs in parallel
- Single P channel power MOSFET
- Two P channel power MOSFETs in parallel

The efficiency of the Converter is defind in equation 1,

$$Efficiency = \frac{Output \quad Power}{Total \quad Input \quad Power} \tag{1}$$

Where,
Output Power =Total input power-Total Power losses (2)

Power loss in the MOSFET is given by

Power Loss = switching loss(P_{sw}) + Conduction loss(P_{con})(3)

Where $P_{sw} = \frac{V_{in} \times I_{in}}{2}\left(T_{rise} \times T_{fall}\right)F_{sw}$ (4)

$$P_{con-loss} = I_{out}^2 \times R_{ds(on)} \times \frac{V_{out}}{V_{in}} \tag{5}$$

Based on the experimental results, loss estimation is shown for Single NMOS Device, with following parameters

$Rds(on)$=0.036Ω; I_{in}=4.79A; V_{in}=14.39V, I_{out}=4.89A, V_{out_t} = 12.27V, F_{SW} = *1000Hz*; T_{rise} = *200µs*; T_{fall} = *5µs*;

$$P_{sw} = \left(\frac{14.39 \times 4.89}{2}\right) \times (200 + 5)us \times 1000\ HZ$$

$$P_{sw} = 7.21\ Watts$$

$$P_{con\_loss} = 4.89^2 \times .036 \times \frac{12.27}{14.39} = .734\ Watts$$

$$P_{efficiency} = \frac{12.27 \times 4.89}{14.39 \times 4.79} = .870 = 87\%$$

System shown in figure 5 is used for converter analysis. Duty cycle is kept constant for all cases. At lower frequencies, conduction period of MOS devices is more compared to conduction period at high frequencies. Therefore efficiency of converter with two NMOS devices is lowered at lower frequencies due to combined conduction losses of two devices. PMOS devices provide comparable efficiency with simple gate driving circuit. Figure 10 shows switching frequency of 1MHz provides best efficiency for the converter.

Maximum current flow is achieved with maximum duty cycle for NMOS device. Results of this analysis are shown in figure 10 and listed in Table 3. Measurements are taken under frequently varying atomspheric conditions such as cloudy and sunny environment. For PMOS devices, maximum current flow

occurs for minimum duty cycle.

Table 3 Experimental Measurements

Solar panel voltage (V)	Solar panel current (A)	Battery voltage (V)	Battery current (A)	Duty cycle %
18.2	1.7	12.7	1.62	40
19.4	0.58	12.6	0.53	50
18.8	1.64	13.4	1.56	60
16.6	1.88	13.09	1.75	70
15.4	2.09	13.3	1.95	80
14.6	2.25	13.3	2.09	90

V. EXPERIMENTAL SET-UP AND FPGA BASED CONTROLLER IMPLEMENTATION

A. Experimental Set-up

Experimental set-up used to analyze converter performance is shown in figure 11. Zero voltage switching signals of drain current with V_{ds} and PWM signal is shown in figure 12 and 13. Switching frequency of 1 MHz with 95% duty cycle is chosen for power MOSFET.

B. FPGA based controller

Spartan 6 FPGA is used to generate switching signal and control battery charging. It is programmed to generate PWM signal of 1MHz switching frequency with 95% duty cycle, for maximum efficiency of converter with single NMOS device.

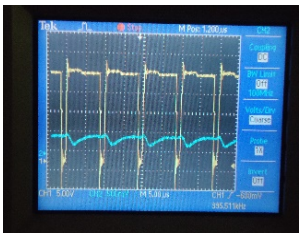

Fig. 12 V_{ds} and I_d

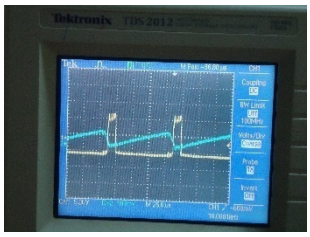

Fig.13 PWM and I_d

Switching signal generation is based on battery charge status. So it senses battery voltage to decide battery status. Following battery parameters are considered for controller design.

1. Open-circuit voltage after full charge: 12.6-12.8V
2. Open-circuit voltage after full discharge: 11.8-12.0V
3. Loaded at full discharge: 10.5V
4. Float charging: 13.8V for gelled and 13.4V for wet cells
5. Typical (daily) charging: 14.2-14.5V

Based on the above parameters, controller set points are decided to connect /disconnect battery with solar panel/ load for charging/discharging. It prevents the battery from over charging / discharging and improves the life of battery. Set points are defined as follows.

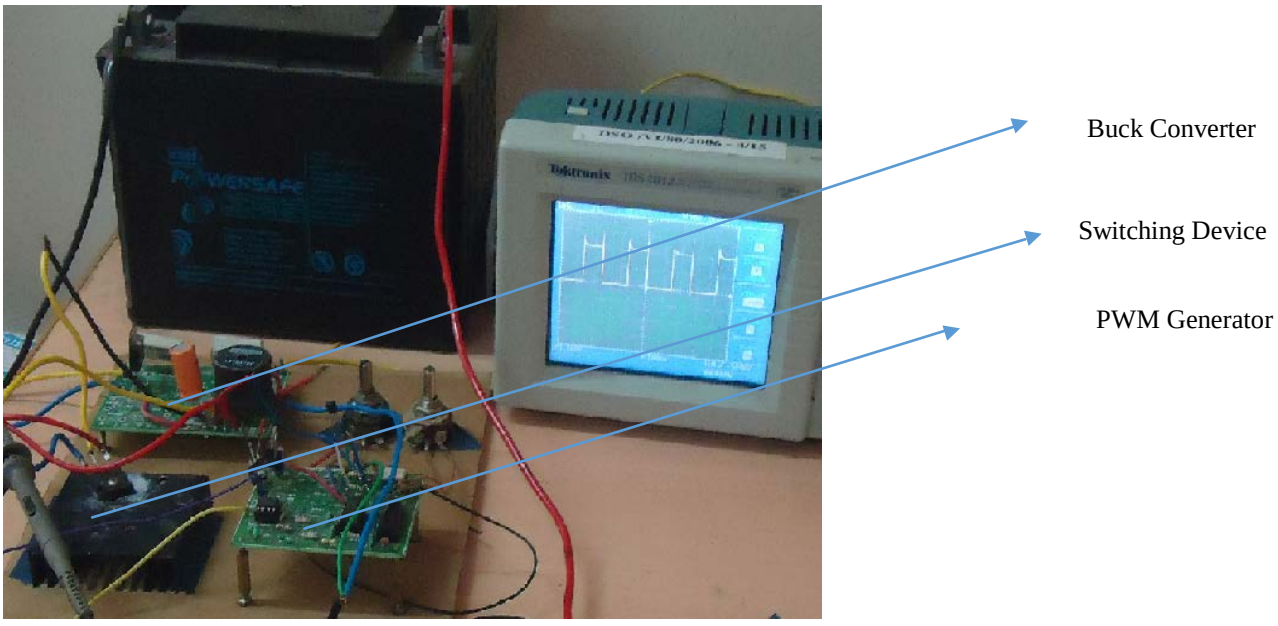

Figure.11 Experimental Set-up

High voltage solar disconnect (HVD) : 14.3V

Battery is disconnected from solar panel (Battery is fully charged) and Load is connected with battery.

High voltage solar reconnect (HVR) : 13.3V

Battery is connected with solar panel for charging at no load

Low voltage load disconnect (LVD) : 11.0V

Load is disconnected from battery (Battery is fully discharged) and Battery is connected with solar panel

Load reconnect voltage (LVR) : 12.75V

Load is connected with battery and Battery is connected with solar panel

Spartan 6 FPGA XC6SLX45-3CSG324C is chosen for controller implementation. Operating clock frequency of Spartan 6 FPGA is 50MHz, it is down converted to 1MHz to supply switching signal of converter with 95% duty cycle. Battery voltage is sensed by FPGA by potential divider voltage sensor and Analog to Digital converter. Flow chart of the FPGA program execution is shown in figure 14. FGPA Hardware utilization of this program is less than 1% of resources and it is chosen to improve the control architecture for automatic PWM generation for better efficiency, according to the type of device and converter [24] with improved battery charging algorithm.

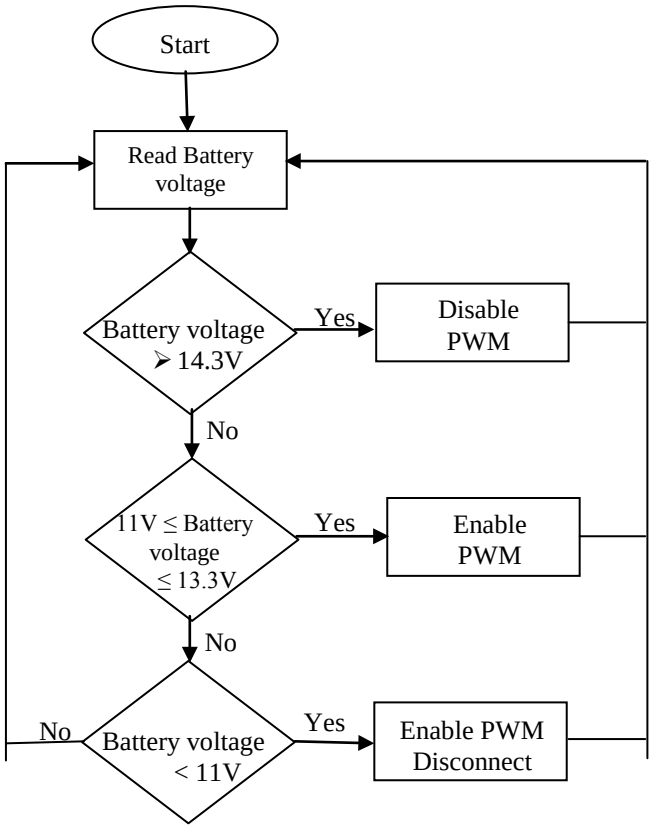

Figure 14 Flow chart of battery charge controller

VI. Conclusion

Power electronic components play vital role in the performance of converters. This paper analyzes various MOSFET configurations in PV battery charger. Results show choosing PMOS device with low on-resistance delivers better performance with simple control circuit. N channel MOS devices operate at maximum effeciency with complex driving circuit. Based on the experimental results, a controller is designed to generate switching signal for efficient battery charging and controls the load. Controller is implemented using Spartan 6 FPGA. More intelligence can be incorporated by including temperature compensation, variable PWM signal generation according to type of power MOSFET for maximum efficiency and extend the controller algorithm for multi-level systems. ASIC implementation of controller enables the developmemnt of module integrated converters.

References

[1] M.Veerachary, T. Senjyu and K. Uezato, "Voltage based Maximim Power Point Tracking Control of PV System", *IEEE Trans. on Aerospace and Electronic systems*, vol. 38, issue 1, 2002, pp. 262-210.

[2] S. Armstrong, W.G. Hurley, "Self-Regulating Maximum Power Point Tracking For Solar Energy Systems", presented in 39th International Universities Power Engineering Conference, vol. 1,2004, pp. 604-609.

[3] S. Armstrong, W.G Hurley, "Investigating the effectiveness of Maximum Power Point Tracking for a Solar System", presented in Power Electronics Conference, 2005, pp. 204-209.

[4] Jonathan W. Kimball and Philip T. Krein, "Discrete-Time Ripple Correlation Control for Maximum Power Point Tracking", *IEEE Transactions on Power Electronics*, vol. 23, issue 5, 2008, pp. 2353-2362.

[5] Qiang Mei, Mingwei Shan, Liying Liu, and Josep M. Guerrero, "A Novel Improved Variable Step-Size Incremental-Resistance MPPT Method for PV Systems", *IEEE Transactions on Industrial Electronics*, vol.58, issue 6, 2011, pp.- 2427-2434.

[6] Trishan Esram, and Patrick L. Chapman, "Comparison of Photovoltaic Array Maximum Power Point Tracking Techniques", *IEEE Transactions on Energy Conversion*, vol. 22, issue 2, 2007, pp. 439-449.

[7] Nabil Karami, Nazih Moubayed and Rachid Outbib, "Analysis of an irradiance adaptive PV based battery floating charger", presented in IEEE Photo-voltaic specialists conference, 2011

[8] Hemza Saidi and Abdelhamid Mudoun, "Improvement of Power Management System in Electro-Solar Vehicle", presented in Advances in Environmental Sciences, Development and Chemistry, CSCC 14, 2014, pp. 286-300.

[9] Naoufel Khaldi, Hassan Mahmoudi, Malika Zazi, Youssef Barradi, "Modelling and Analysis of Neural Network and Perturb and Observe MPPT Algorithm for PV Array Using Boost Converter", presented in Modelling and Systems, CSCC 14, 2, 2014, pp. 651-655.

[10] Penin Alexander, "Analysis of regimes of voltage regulators with limited capacity voltage", *Wseas Transactions on Circuits and Systems*, vol. 1, 2013, pp. 1-12.

[11] Antonio M. P. Lucena, Paulo D. L. Oliveira, Clauson S. N. Rios, Magno P. Almeida Filho, and Francisco de A. T. F. da Silva, "Flexible FPGA-based BPSK Signal Generator for Space Applications", *Naun Transactions on International Journal of Circuits, Systems and Signal Processing*, vol. 8, 2014, pp. 160-165.

[12] Cheng Sen, Zhao Ping, He Hongkun, Ji Qianqian, and Wei Xu, "An Improved Design of Photo-Voltaic Solar Tracking System Based on FPGA", presented in International Conference on Artificial Intelligence and Computational Intelligence, 2010, pp. 267-271.

[13] B. Chitti Babu, Sriharsha, Ashwin Kumar, Nikhil Saroagi and S.R.Samantaray, "Design and Implementation of Low Power Smart PV Energy System for Portable Applications using Synchronous Buck Converter", presented in International Symposium on Electronic System Design, 2011.

[14] L. Huber, K. Hsu, M. M. Jovanovic, D. J. Solley, G. Gurov and R. M.Porter, "1.8-MHz, 48-V resonant VRM: Analysis, design, and performance evaluation", *IEEE Trans.on Power Electron.*, vol. 21, issue 1, 2006, pp. 79–88.

[15] Y. Ren, K. Yao, M. Xu and F. C. Lee, "Analysis of the power delivery path from the 12-V VR to the microprocessor", *IEEE Trans. on Power Electron.*, vol. 19, issue 6, 2004, pp. 1507–1514.

[16] Drazen Dujic, Gina K. Steinke, Bellini, Munaf Rahimo Liutauras Storasta, and Juergen K. Steinke, "Characterization of 6.5 kV IGBTs for High-Power Medium-Frequency Soft-Switched Applications", *IEEE Transactions on Power Electronics*, vol. 29, issue 2, 2011, pp. 906-919.

[17] Shahram Javadi, Mehrnaz Fard Amiri, "A Fuzzy based controller for Wind Energy Conversion System using PWM CSI diode Rectifier and Buck Converter, presented in Advances in Robotics, Mechatronics and Circuits, CSCC 14, 277-282, 2014.

[18] M.B.I Reaz, J.Jalil, H.Husain, F.H.Hashim, "FPGA Implementation of Elliptic Curve Cryptography Engine for personal Communication Systems", *Wseas Transactions on Circuits and Systems*, vol. 3, 2012, pp. 82-91.

[19] Jean-Christophe Crebier and Nicolas Rouger, " Loss Free Gate Driver Unipolar Power Supply for High Side Power Transistors", *IEEE Transactions on Power Electronics*, vol. 23, issue 3, 2008, pp. 1565-1573.

[20] Tse-Ju Liao, Chia-Chieh Hung, Chern-Lin Chen, "Source switching circuit with low-gate-driving loss in high-voltage buck light emitting diode driver", *IET Power Electronics*, vol. 6, 2013, pp. 663-671.

[21] Trevor A.Smith, Sima Dimitrijev and H. Barry Harrison, "Controlling a DC-DC converter by Using a Power MOSFET Voltage Controlled Resistor", *IEEE Transaction on Circuits and Systems*, vol. 47, issue 3, 2008.

[22] Zhiliang Zhang, Fei-Fei Li, and Yan-Fei Liu, "A High-Frequency Dual-Channel Isolated Resonant Gate Driver With Low Gate Drive Loss for ZVS Full-Bridge Converters", *IEEE Transactions on Power Electronics*, vol. 29, issue 6, 2104, pp. 3077-309.

[23] Kamala. J, Janarthanan. V, and Santhosh. K, Performance Measure of Switching Device (MOSFET) in Photo-voltaic System, presented in International Conference on Circuts, Systems, Communications and Computers (CSCC 2014), July 17-21, 2014.

[24] Juan Paulo Robles Balestero, Fernando Lessa Tofoli, Grover Victor Torrico-Bascope and Falcondes Jose Mendes de Seixas, "A DC–DC Converter Based on the Three-State Switching Cell for High Current and Voltage Step-Down Applications", *IEEE transactions on power electronics*, vol. 28, issue 1, 2013.